AUS DEM LEHRSTUHL FÜR AUGENHEILKUNDE
PROF.DR.HORST HELBIG
DER FAKULTÄT FÜR MEDIZIN
DER UNIVERSITÄT REGENSBURG

UNTERSUCHUNG MOLEKULARER GRUNDLAGEN DER BESTROPHIN-1-/Ca^{2+}-KANAL-INTERAKTION

Inaugural – Dissertation
zur Erlangung des Doktorgrades
der Medizin

der Fakultät für Medizin
der Universität Regensburg

vorgelegt von
Nadine Reichhart

2012

AUS DEM LEHRSTUHL FÜR AUGENHEILKUNDE
PROF.DR.HORST HELBIG
DER FAKULTÄT FÜR MEDIZIN
DER UNIVERSITÄT REGENSBURG

UNTERSUCHUNG MOLEKULARER GRUNDLAGEN DER BESTROPHIN-1-/Ca^{2+}-KANAL-INTERAKTION

Inaugural – Dissertation
zur Erlangung des Doktorgrades
der Medizin

der Fakultät für Medizin
der Universität Regensburg

vorgelegt von
Nadine Reichhart

2012

Dekan:	Prof. Dr. Dr. Torsten E. Reichert
1. Berichterstatter:	Prof. Dr.rer.nat. Olaf Strauß
2. Berichterstatter:	Prof. Dr.rer.nat. Rainer Schreiber
Tag der mündlichen Prüfung:	11.03.2013

Experimental Eye Research 91 (2010) 630–639

Contents lists available at ScienceDirect

Experimental Eye Research

journal homepage: www.elsevier.com/locate/yexer

Effect of bestrophin-1 on L-type Ca^{2+} channel activity depends on the Ca^{2+} channel beta-subunit

Nadine Reichhart [a], Vladimir M. Milenkovic [a], Claire-Amelie Halsband [b], Sönke Cordeiro [c], Olaf Strauß [a,*]

[a] Experimental Ophthalmology, Eye Hospital, University Medical Center Regensburg, Franz-Josef-Strauß Allee 11, 93053 Regensburg, Germany
[b] Department of Neurology, Klinikum rechts der Isar, Munich, Germany
[c] Institut für Neurophysiologie, Medizinische Hochschule Hannover, Hannover, Germany

ARTICLE INFO

Article history:
Received 27 March 2010
Accepted in revised form 2 August 2010
Available online 7 August 2010

Keywords:
$Ca_V1.3$ subunits
β-subunits
bestrophin-1
L-type channels
retinal pigment epithelium

ABSTRACT

Best's vitelliforme macular degeneration is an inherited retinal degeneration associated with a reduction of the light-peak in the patient's electro-oculogram. Bestrophin-1, the product of the disease-promoting/forming gene can function as regulator of voltage-dependent L-type Ca^{2+} channels in the retinal pigment epithelium (RPE). Since mice deficient for either β4-subunits or $Ca_V1.3$ subunits show reduced light-peaks, the regulatory function of bestrophin-1 on heterologously expressed Ca^{2+} channels composed of the pore-forming $Ca_V1.3$ and the auxiliary β4-subunit was analyzed. Precipitation of β4-subunits led to co-precipitation with bestrophin-1 and subsequent analysis of subcellular localization showed co-localization of bestrophin-1, $Ca_V1.3$ and β4-subunit in the cell membrane. $Ca_V1.3$ currents in the presence of β4-subunits and bestrophin-1 showed accelerated time-dependent activation and decreased current density compared to currents measured in the absence of bestrophin-1. In the presence of the β3-subunit, which is not expressed in the RPE bestrophin-1 did not modulate $Ca_V1.3$ activity. Deletion of a cluster of proline-rich motifs in the C-terminus of bestrophin-1 reduced its co-immuno precipitation with the β4-subunit and strongly reduced the $Ca_V1.3$ activity. Cells co-expressing bestrophin-1 lacking the proline-rich motifs and $Ca_V1.3$ subunits showed less efficient trafficking of bestrophin-1 into the cell membrane. In summary, we conclude that bestrophin-1 modulates L-type channels of the RPE via proline-rich motif-dependent interaction with β4-subunits. A disturbed interaction reduces the currents of the $Ca_V1.3$ subunits. This mechanism could open new ways to understand changes in the patient's electro-oculogram and functional alterations of the RPE leading to retinal degeneration.

1. Introduction

Best's vitelliforme macular dystrophy is rare autosomal inherited retinal degeneration, with a juvenile age of onset, and is caused by altered function of the retinal pigment epithelium (RPE) (Best, 1905; Boon et al., 2009). Hallmarks of the disease are a fast accumulation of lipofuscin and a decreased light-peak in the electro-oculogram (EOG). The product of the gene which causes Best's disease, bestrophin-1 (Marquardt et al., 1998; Petrukhin et al., 1998), has been described to modulate the function of a Cl^- channel and voltage-dependent L-type Ca^{2+} channels (Hartzell et al., 2008). The RPE interacts closely with the photoreceptors and fulfills many of the tasks required to maintain visual function (Strauss, 2005). Thus the clinical picture results from a disturbance of the RPE function caused by mutant bestrophin-1.

The ability of bestrophin-1 to modulate Ca^{2+} channel activity suggests a mechanism with which to understand/or explain? the decreased light-peak in the patient's EOG. The RPE expresses $Ca_V1.3$ channels and auxiliary β2- and β4-subunits of voltage-dependent Ca^{2+} channels (Wimmers et al., 2008). The public SAGE database also indicates the expression of β1-subunits in the RPE. Systemic application of nimodipine, an L-type channel blocker, led to a reduction of the light-peak amplitude as assessed using rat or mouse direct-current (DC-)electroretinograms (Marmorstein et al., 2006; Rosenthal et al., 2006). This pharmacological evidence is also supported by genetic mouse models, as $Ca_V1.3$ knock-out mice also showed decreased light-peak amplitude (Wu et al., 2007). Furthermore, "lethargic mice", which do not express Ca^{2+} channel β4-subunits, showed decreased light-peak amplitude, whereas β2-subunit knock-out mice showed no changes in the light-peak (Marmorstein et al., 2006). Thus the light-peak is generated by

* Corresponding author. Tel.: +49 941 944 9228; fax: +49 941 944 9202.
E-mail address: strauss@eye-regensburg.de (O. Strauß).

0014-4835/$ – see front matter © 2010 Elsevier Ltd. All rights reserved.
doi:10.1016/j.exer.2010.08.001

the involvement of $Ca_V1.3$ Ca^{2+} channels in combination with β4-subunits in the RPE (Marmorstein et al., 2006; Wu et al., 2007). Furthermore, basic functions of the RPE are associated with the activity of L-type Ca^{2+} channels (Wimmers et al., 2007). For example, L-type channel activity regulates the secretion of vascular endothelial growth factor (Rosenthal et al., 2007), as well as phagocytosis of photoreceptor outer membranes (Karl et al., 2008). Thus, the understanding of altered regulation of L-type channels by mutant bestrophin-1 would help to understand the effects of these mutations on RPE function.

The pore-forming $Ca_V1.3$ subunit corresponds with the a1D subunit or the neuroendocrine L-type channel (Striessnig, 1999). The $Ca_V1.3$ channel is expressed in RPE cells would be therefore the natural target of bestrophin-1-dependent regulation (Rosenthal et al., 2006). Over-expression of bestrophin-1 in RPE cells, which endogenously express L-type channels of the $Ca_V1.3$ subtype, leads to a shift in the voltage-dependent activation towards more negative membrane potentials, and to an acceleration of the time-dependent activation (Rosenthal et al., 2006). Mutant forms of bestrophin-1, W93C and R218C, mainly led to changes in the kinetic behavior of the channels (Rosenthal et al., 2006). Comparable observations were made with heterologously expressed $Ca_V1.2$ channels, which correspond with the cardiac subtype of L-type channels, and bestrophin-1 (Burgess et al., 2008). Here, also time-dependent activation was accelerated by bestrophin-1. However, voltage-dependence was not investigated. Mutant bestrophin-1, R141H, showed a loss of function effect and failed to modulate Ca^{2+} channel activity (Burgess et al., 2008). In a third study using heterologously expressed rat $Ca_V1.3$ and bestrophin-1, inhibition of the $Ca_V1.3$ channel currents and a shift of the voltage-dependent activation towards more positive membrane potentials were observed (Yu et al., 2008). More importantly, this study could identify a mechanism which enables the modulation of Ca^{2+} channel activity by bestrophin-1, namely that bestrophin-1 binds to Ca^{2+} channel β-subunits via an interaction between an SH3-domain of the β-subunit and proline-rich motifs on the C-terminus of bestrophin-1. Thus the reported effects of bestrophin-1 on L-type channel activity, for reasons that are unclear to date, are inconsistent. Possible reasons could be the different experimental conditions such as the expression of different Ca^{2+} channel Ca_V1 subunits: rat versus human, usage of different clones, $Ca_V1.3$ versus $Ca_V1.2$ or endogenously expressed channels versus over-expressed channels. In addition to that all studies to date have employed different auxiliary β-subunits.

Therefore, the aim of the study was to investigate the functional impact of β-subunits on bestrophin-1-dependent modulation of L-type channel activity in an isolated system. This was achieved using CHO and HEK cells as the expression systems (although some results were confirmed in ARPE-19 cells). Since the most prominent effect of L-type channel activity on light-peak amplitude was observed in "lethargic mice" (Marmorstein et al., 2006), we concentrated our study on the β4-subunit. For comparison β3-subunits, which are not known to be expressed in the RPE (Wimmers et al., 2008), were chosen as an additional control. The interaction of either β-subunit with bestrophin-1 has not been investigated to date. We chose to study the bestrophin-1-dependent modulation of the human $Ca_V1.3$ subunit as it has been shown to be the predominant L-type channel in the RPE (Wimmers et al., 2007). By means of protein biochemistry and electrophysiology of heterologously expressed $Ca_V1.3$ subunits, and bestrophin-1, we discovered that interaction between the β4-subunit and bestrophin-1 modulates L-type channels currents. This interaction was specific to the β4-subunit, as no effect of bestrophin-1 in the presence of the β3-subunit was observed on L-type channels currents.

2. Materials and methods

2.1. Cell culture

To study protein/protein interaction in an isolated system by means immunoprecipitation HEK cells were chosen because of their high expression rates. For L-type channel current analysis CHO cells were chosen because these cells are better suitable for microinjection. Trafficking properties were analyzed in ARPE-19 cells because these cells display the special protein trafficking characteristics of RPE cells. Cell culture and transduction – CHO (ATCC, cat# CCL-61) cells were cultured in 100-mm culture dishes in Ham's F-12 medium (Invitrogen). HEK-293 cells (ATCC, cat# CRL-1573), were cultured in Dulbecco's modified Eagle's medium (D-MEM) medium containing L-glutamine, 4500 mg/l glucose and 110 mg/l sodium pyruvate. ARPE-19 (ATCC, cat# CRL-2302) cells were cultured in DMEM/Ham's F-12 medium, 50:50 mixture supplemented with insulin/transferin, nonessential amino acids, and 15 mM HEPES buffer (Invitrogen). All media were supplemented with 10% (v/v) fetal calf serum (Invitrogen), and 1% (v/v) penicillin-streptomycin (Invitrogen). Cells were cultured at 37 °C, with relative humidity of 95% and 5% CO_2 concentration.

Plasmid Constructs – 1. Human bestrophin-1, BEST-1 [Homo sapiens; NM_004183], hBest-pcDNA3.1 2. calcium channel, voltage-dependent, β3 (Rattus norwegicus; NM_012828), and β4-subunit [Rattus norvegicus; Gene ID 25297 and 58942]; depending on experimental conditions tagged either His or (c-Myc) β3-pCMV, and β4-pCDNA3; 3. Cacna1d, calcium channel, voltage-dependent, L-type, α1D subunit $Ca_V1.3$ (Homo sapiens: NM_000720.2); 4. α2δ–pcDNA3 (Gene ID 776), 5. eGFP pcDNA3 reporter plasmid was used as transduction control. Ca^{2+} channel constructs were provided by Prof. Striessnig (Innsbruck). Human bestrophin-1 constructs were provided by Prof. Weber (Regensburg). All described constructs were sequenced for integrity, and pure plasmid DNA was isolated by using a plasmid maxi kit (Qiagen). Deletion of the proline-rich region (320–350aa) was introduced into human bestrophin-1 by PCR using the following primers: 5′-ACGGGTACCCCACCATGACCATCACTTACACA; 5′-CGTACCGGTGGAATGTGCTTCATCCCT; 5′-AGGAATTTGCAGGTGTCCCTGGAATTCTCA; 5′-GTGCATCTCATCCACAGCCAAGAATTCTGA. Resulting PCR product was digested using KpnI/EcoRI and EcoRI/AgeI restriction enzymes, and subsequently inserted into pCDNA3-bestrophin-1 plasmid digested with KpnI/AgeI. 30 amino acids (320–350aa) were deleted. All the constructs were verified by DNA sequencing.

2.2. Heterologeous expression of L-type channels and bestrophin

2.2.1. Transduction

For precipitation experiments subconfluent HEK-293 (70–80%) cells were transiently transduced with Ca^{2+} channel subunits and human bestrophin-1. All transductions were carried out using Satisfection transduction reagent (Stratagene) following the manufacturer's instructions. Cells were analyzed at 36 h after transduction.

2.2.2. Microinjection

For patch-clamp experiments and confocal microscopy CHO cells were microinjected because the successful investigation of L-type channels currents under influence of bestrophin-1 requires the presence of the four plasmids for $Ca_V1.3$, β-subunit, α2δ-subunit and bestrophin-1 itself. The presence of all four proteins was confirmed after every patch-clamp experiment by immuno histochemistry. Microinjections were performed under an inverted microscope (Carl Zeiss) equipped with a micromanipulator InjectMan NI2 (Eppendorf) by using an automated FemtoJet (Eppendorf)

and Femtotip (Eppendorf) glass microcapillaries. CHO cells were plated on 12-mm glass plates and microinjected with plasmid DNA (50 ng/μl for each construct). Immediately after microinjection, cells were incubated overnight at 30 °C, and next day cells were transferred into 37 °C cell culture incubator.

2.3. Precipitation and Western-blotting of Ca^{2+} channel proteins and bestrophin-1

Subconfluent (70–80%) culture of HEK-293 cells were transiently transduced with combinations of plasmids encoding either (a) bestrophin-1 and β3-6His or (b) bestrophin-1 and β4-6His subunits of voltage-dependent calcium channels using Satisfaction transduction reagent (Stratagene) according to the manufacturer's protocol. The pEGFP plasmids were used as negative control. After a 36-h incubation, cells were washed with 1× PBS and then lysed in culture dish with shaking for 15 min at 4 °C with ice-cold lysis buffer (150 mM Tris–HCl, pH 7.5, 150 mM NaCl, 1% Nonidet-P40, 0.5% natrium deoxycholate). Cell lysate was scraped and transferred to a new tube and lysed for additional 15 min at 4 °C with rocking. The lysates were clarified by centrifugation at 13,000 × g for 10 min at 4 °C.

Supernatants were applied to 50 μl of Protein G-Agarose (Roche) and incubated 3 h with rocking at 4 °C. After pre-clearing and centrifugation at 13,000 × g for 1 min the lysates were applied to new tubes with 50 μl of HisPur Cobalt Resin (Pierce). After overnight incubation on a rotating wheel at 4 °C the beads were washed three times with washing buffer (50 mM Tris–HCl, pH 7.5, 150 mM NaCl, 1% Nonidet-P40, 0.5% natrium deoxycholate, 10 mM imidazole). All centrifugation steps were carried out at 1200 × g for 1 min at 4 °C.

Protein complexes were dissociated from beads by incubation at 90 °C for 3 min in 4×SDS loading buffer with 150 mM imidazole. The precipitates were subjected together with total lysates to 10% SDS-PAGE and Western-blot was carried out. The proteins were blotted to PVDF filter membranes (GE Healthcare), and blocked in 5% nonfat dry milk. After incubation with primary antibodies, blots were visualized with peroxidase-conjugated secondary antibodies (New England Biolabs) and a enhanced chemiluminiscence (ECL) kit (Pierce) according to manufacturer's instructions. The images were digitalized using an image analyzer (Chemimager, Biozym).

2.4. Antibodies

Proteins were detected by mouse monoclonal anti-human bestrophin-1, ab2182, (Abcam plc), anti-bestrophin-1 antibody (kindly provided by Prof. Dr. Karl Kunzelmann), rabbit anti-Ca_VBeta3 (Alomone Labs), goat anti Ca_V1.3 (Santa Cruz), mouse anti-c-Myc (9E10)(Developmental Studies Hybridoma Bank), rabbit anti-6His, ab9108, (Abcam plc), mouse monoclonal anti-GFP (Roche) followed by incubation with the HRP-conjugated goat anti-rabbit or goat anti-mouse antibodies (New England Biolabs).

Immunohistochemistry and confocal microscopy – Microinjected CHO cells were grown on a sterile glass cover slip. Thirty-six hours after the microinjection cells were washed with 1× PBS, and fixed for 10 min at room temperature with 4% (w/v) para-formaldehyde. After three additional washing steps with 1× PBS, cells were permeabilized with blocking/permeabilization solution [10% (v/v) normal goat serum, 0.5% (v/v) Triton X-100 in 1× PBS] for 30 min. Cells were then labeled for overnight with anti-bestrophin antibody, ab2182, (Abcam plc), goat anti Cav1.3 (Santa Cruz), and anti-β3 antibody (Alomone Labs) diluted 1:500 in 2% normal goat serum, 0.1% Triton X-100 in 1× PBS. After three additional washing steps cells were incubated for 1 h with appropriate secondary antibodies conjugated with Alexa 488, Alexa 546, and Alexa 633 (Invitrogen). Cells were mounted in confocal matrix (Micro Tech Lab) and then examined using confocal microscope LSM510 (Carl Zeiss). Triple fluorescence for green, red and infrared channels was obtained using excitation of an argon–helium–neon laser at wave lengths of 488, 546, and 633 nm. Single X–Y optical sections were obtained by sequential scanning for each channel to eliminate the crosstalk of chromophores and to ensure reliable quantification of co-localization. Images were recorded at intensity levels bellow saturation, estimated by intensity analysis module. Confocal images were quantitatively analyzed using an ImageJ software package (Abramoff et al., 2004). Pearson's correlation coefficient (PCC) was employed to evaluate co-localization.

2.5. Patch-clamp recordings of L-type channel currents

Membrane currents were measured in the whole-cell configuration of the patch-clamp technique. During the recordings transfected cells were superfused by a bath solution containing (mM): choline chloride 150, $BaCl_2$ 10, $MgCl_2$ 1, HEPES 10; pH 7.4 adjusted with CsOH; 333mOsm. The perfusion chamber was mounted onto a stage of an inverted fluorescence microscope. Transfected cells were selected by their GFP fluorescence. For whole-cell recording patch-pipettes of 3–5 MΩ were made from borosilicate tubes using a DMZ-Universal Puller (Zeitz). Pipettes were filled with a pipette-solution containing (mM): CsCl 135, $MgCl_2$ 1, CsEGTA 10; pH 7.4 adjusted with CsOH; 283 mOsm. Membrane currents were recorded using an EPC-10 computer-controlled patch-clamp amplifier in conjunction with the software TIDA for data acquisition and analysis. The mean membrane capacitance was 22.04 ± 1.3 pF ($n = 25$). The access resistance was compensated for to values lower than 10 MΩ. For analysis of voltage-dependent activation steady-state currents were plotted against the membrane potentials of the electrical stimulation. Plots of each individual cell were fitted using the Boltzmann equation.

2.6. Statistical analysis

Statistical significance was tested using one-way analysis of variance (ANOVA). All data were given as mean ± SEM. n = number of independent experiments, * = statistical significance with $p < 0.05$. Mean values of data obtained from Boltzmann fits calculated for each individual cell.

3. Results

3.1. Regulation of L-type channels by bestrophin-1 involves interaction with β4-subunits

Co-expression of Ca_V1.3 together with α2δ and β4-subunits resulted in characteristic L-type channels currents (Fig. 1A) which were comparable to those in other studies (Table 1). The currents activated at membrane potentials more positive than −40 mV with a voltage of half-maximal activation of −24.5 ± 0.7 mV (Fig. 1C, E; $n = 11$). With the β4-subunit at +20 mV the activation time constant was at 2.2 ± 0.26 ms (Fig. 1D; $n = 11$) and the maximal current density was 14.7 ± 2.2 $pApF^{-1}$ (Fig. 1F; $n = 11$). The presence of bestrophin-1 led to changes in the L-type channel characteristics (Fig. 1B, D, F). The voltage-dependent activation remained unchanged (Fig. 1E). The current density was with 8.9 ± 1.4 $pApF^{-1}$ significant smaller ($p = 0.01$, $n = 14$; Table 1) and the time-dependent activation of the currents was accelerated by two times at voltages between 0 and +20 mV (Table 1). At the membrane voltage +20 mV the time activation constant was 1.3 ± 0.18 ms ($n = 14$; $p = 0.0025$) with bestrophin-1 significantly faster than 2.2 ms without bestrophin-1.

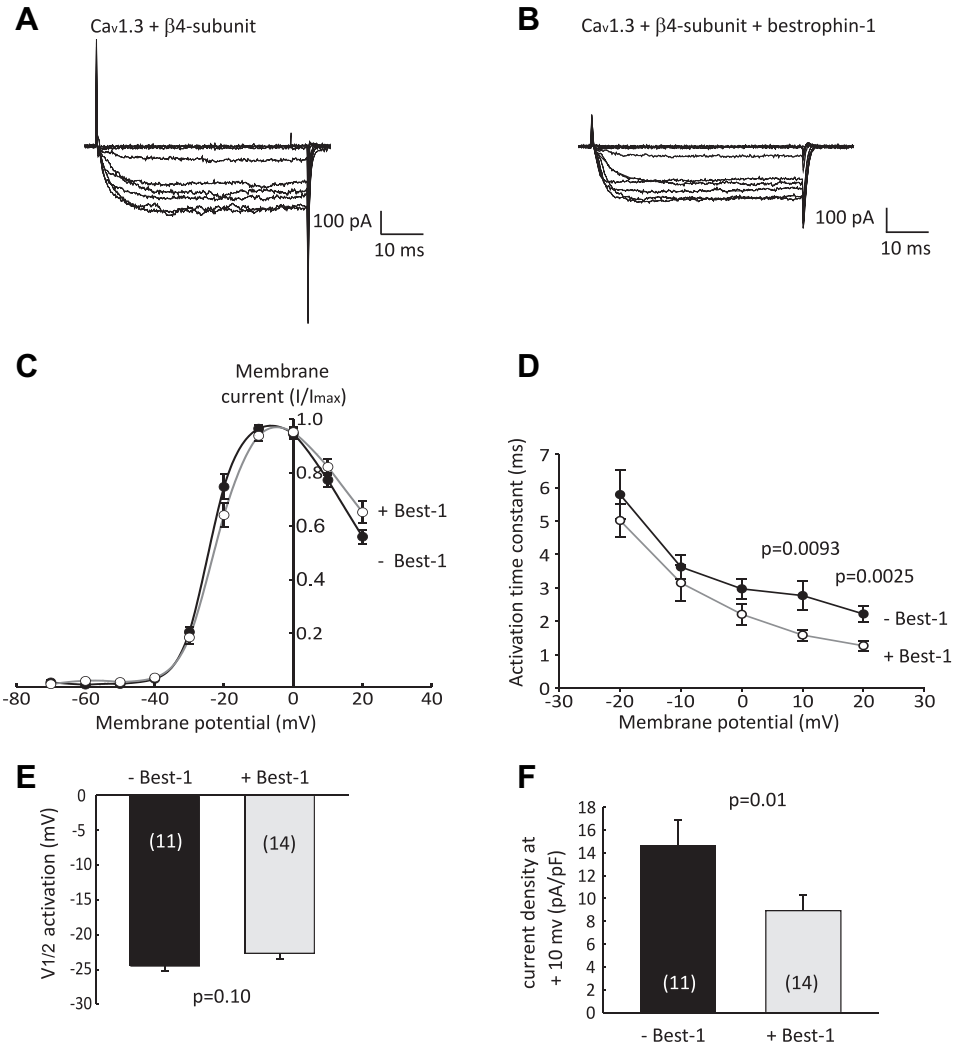

Fig. 1. Whole-cell currents of heterologously expressed L-type channels with β4-subunits in CHO cells. 1A: Ba^{2+} currents through $Ca_V1.3$ subunits ($Ca_V1.3$ subunit, β4-subunit, α2δ-subunit); electrical stimulation by depolarization from a holding potential of −70 mV by nine voltage-steps with +10 mV increasing amplitude and 50 ms duration. 1B: Ba^{2+} currents through $Ca_V1.3$ subunits with bestrophin-1 ($Ca_V1.3$ subunit, β4-subunit, α2δ-subunit, bestrophin-1); electrical stimulation as in 1A. 1C: Analysis of voltage-dependent activation: steady-state current amplitudes in the presence or absence of bestrophin-1 were plotted against the potentials of the electrical stimulation; curves were fitted using the Boltzmann equation, 1D: Analysis of time-dependent activation: time-dependent activation was measured by single exponential fit of the current activation in the presence or absence of bestrophin-1 and plotted as activation time constant over membrane potential. 1E: Comparison of voltage-dependent activation as potential of half-maximal activation (calculated from Boltzmann fits) in the presence and the absence of bestrophin-1. 1F: Comparison of maximal current density in the presence or absence of bestrophin-1. (numbers in columns: the number of experiments).

The electrophysiological investigation of heterologously expressed L-type channels revealed that bestrophin-1 has specific effects on L-type channel activity which probably result from interaction with Ca^{2+} channel proteins. Thus Ca^{2+} channel proteins were expressed in HEK-293 cells and precipitation experiments were conducted to investigate protein–protein interaction (Fig. 2). According to previous publications we concentrated on interaction of bestrophin-1 and β-subunits. Cells were double transfected with bestrophin-1, and β4-subunits His-tagged. Lysates were prepared from these cells and β4-subunits were precipitated from this lysate using cobalt-beads which bind to the His-tag. Precipitates were then analyzed by Western-blot for β4-subunits (55 kDa) and for proteins which bind to β4-subunits and can be therefore co-precipitated. In these precipitates bestrophin-1 (67 kDa) was detected together with β4-subunits indicating a co-precipitation between β4-subunits and bestrophin-1 (Fig. 2A and B). In control experiments in the absence β-subunits precipitation of bestrophin-1 showed no unspecific co-precipitation (Fig. 2C and D). To support observations of protein–protein interaction in intact cells, transfected cells were analyzed by immune cytochemistry for co-localization of these proteins as indicator of physical interaction (Fig. 2F and G). In microinjected cells expressing bestrophin-1, $Ca_V1.3$, α2δ and β4-subunits we showed the presence of bestrophin-1, $Ca_V1.3$ and β4-subunits the cell membrane (Fig. 2F). Overlapping fluorescence in merged pictures indicates co-localization of proteins and suggests direct interaction. To quantify this we performed pixel analysis and calculated Pearson's correlation coefficient. Pixel analysis of the fluorescence signals of bestrophin-1 and b4-subunit resulted in a Pearson's correlation coefficient $85.3 \pm 0.76\%$ ($n = 7$) meaning that 85% of the fluorescence signals of the two proteins did overlap. To evaluate the presence of the proteins in the cell membrane fluorescence profiles were measured across the cell in distant areas to the nucleus. In order to quantify the localization of the proteins in the cell membrane the ratio of the fluorescence of the different proteins in the cell membrane and their fluorescence in the cytoplasmic areas was calculated. A ratio of 1 would indicate an equal distribution and ratios above 1 would indicate accumulation of proteins in the cell membrane compared

Table 1
Properties of the L-type Ca^{2+} channel currents elicited by the interaction of the Ca^{2+} channel b3/4-subunits with bestrophin-1/Best-1ΔPxxP.

	Current density at +10 mV ($pApF^{-1}$)	$V_{1/2}$ activation (mV)
β3-subunit ($n = 11$)	9.63 ± 1.83	−19.57 ± 1.18
β3-subunit + bestrophin-1 ($n = 13$)	6.23 ± 1.11	−21.32 ± 3.53
β4-subunit ($n = 11$)	14.65 ± 2.2	−24.49 ± 0.66
β4-subunit + bestrophin-1 ($n = 14$)	8.93 ± 1.41	−22.67 ± 0.83
β4-subunit + Best-1-ΔPxxP ($n = 6$)	4.21 ± 0.62	−20.76 ± 2.2

Activation time constant at certain potentials (ms)					
	+20 mV	+10 mV	0 mV	−10 mV	−20 mV
β3-subunit ($n = 11$)	1.80 ± 0.14	2.18 ± 0.19	2.77 ± 0.24	4.10 ± 0.5	6.24 ± 0.7
β3-subunit + bestrophin-1 ($n = 9$)	2.22 ± 0.31	2.44 ± 0.3	3.63 ± 0.5	4.64 ± 0.77	8.09 ± 2.1
β4-subunit ($n = 11$)	2.21 ± 0.25	2.77 ± 0.42	2.97 ± 0.3	3.62 ± 0.35	5.79 ± 0.74
β4-subunit + bestrophin-1 ($n = 14$)	1.26 ± 0.15	1.58 ± 0.17	2.21 ± 0.3	3.15 ± 0.54	5.01 ± 0.49
β4-subunit + Best-1-ΔPxxp ($n = 6$)	1.3 ± 0.33	1.43 ± 0.27	1.94 ± 0.46	2.56 ± 0.69	3.39 ± 1.23

to the cytoplasmic localization. In these pictures we measured ratios between 2.7 and 4.8 which indicate that the largest amount of these proteins was in the cell membrane.

3.2. Analysis of bestrophin-1 and L-type channel localization in situ and in vitro

Since analysis of heterologously expressed proteins reveal physical interaction of bestrophin-1 and L-type channels the possibility of this interaction was studied in fresh sections of the porcine retina. Staining of the retina for bestrophin-1 revealed the unique expression of bestrophin-1 in the RPE at the basolateral membrane (Fig. 3A). When the retina was stained for $Ca_V1.3$ the same localization was observed. When merging the pictures of the green bestrophin-1 and red $Ca_V1.3$ staining the resulting yellow color of the overlay picture shows direct co-localization of both proteins (Fig. 3B/C). Also in cultured RPE cells the Ca^{2+}-channel proteins and bestrophin-1 are transported into the cell membrane. ARPE-19 cells were transduced with $Ca_V1.3$, β4-subunits and bestrophin-1. Analysis of the subcellular localization of the three proteins by confocal microscopy revealed that all three proteins are localized are in the cell membrane (Fig. 3D). Using pixel analysis of the fluorescence signals of bestrophin-1 and β4-subunits proteins resulted in a Pearson's correlation coefficient 59.7%. Their fluorescence intensities between cell membrane and cytoplasmic localization indicated strong membrane localization with ratios between 3.6 and 4.8.

3.3. Effects of bestrophin-1 on L-type channels composed of β3-subunits and $Ca_V1.3$ subunits

β3-subunits are not expressed by the RPE. Thus effects of bestrophin-1 in the presence of β3-subunits were investigated as control (Fig. 4). First immunoprecipitation experiments were conducted to study possible physical interaction between bestrophin-1 (67 kDa) and β3-subunits (55 kDa). In these precipitates bestrophin-1 was detected by means of Western-blot (Fig. 4A). Staining of the same Western-blot with anti-His antibodies showed all His-tagged β3-subunit (55 kDa) was precipitated (Fig. 4B). Co-expression of $Ca_V1.3$ subunits together with α2δ and β3-subunits resulted in characteristic L-type channel currents (Fig. 4C). The currents activated at potentials more positive than −40 mV (Fig. 4E). The analysis of the voltage-dependent activation by Boltzmann fit resulted in a value for the potential of the half-maximal activation of −19.5 ± 1.2 mV ($n = 11$; Fig. 4E). The activation time constant at the maximal current amplitude was 1.8 ± 0.15 ms ($n = 11$; Fig. 4D), the maximal current density was 9.6 ± 1.8 $pApF^{-1}$ ($n = 11$; Fig. 4F). These current characteristics were not changed in the presence of bestrophin-1 (Fig. 4B, C,D,F). Neither current density (6.2 ± 1.2 $pApF^{-1}$; $n = 13$, $p = 0.12$), activation time constants (at + 20 mV: 2.2 ± 0.3 ms; $n = 13$, $p = 0.37$) nor voltage-dependent activation (voltage of half-maximal activation: −21.3 ± 3.5 mV; $n = 13$, $p = 0.67$) were changed when Ca^{2+} channel subunits were co-expressed with bestrophin-1. However, in cells which have been microinjected with bestrophin-1, $Ca_V1.3$, α2δ and β3-subunits (Fig. 4G) also all three proteins could be detected in the cell membrane (ratios of fluorescence profile between 2.6 and 3.4). A Pearson's correlation coefficient of 63.5% for bestrophin-1 and β3-subunits suggests that a major amount of the three proteins interact.

3.4. Role of proline-rich motifs on the C-terminus of bestrophin-1

In a previous publication it was shown that the modulation of L-type channel activity is mediated by proline-rich motif/SH3-domain interaction. In order to study that the influence of bestrophin-1 via β4-subunits is mediated by the same mechanism we generated a mutant form of bestrophin-1 (Fig. 5, Best-1-ΔPxxP) which lacks a cluster of proline-rich (PxxP) motifs between amino acid position 330 and 346 (the amino acids between 320 and 350 were removed). The removal of this cluster of amino acids did not remove the epitope for the anti-bestrophin-1 antibodies (Fig. 5A). Using this mutant bestrophin-1 immunoprecipitation experiments were conducted from HEK cells which heterologously express β4-subunit c-Myc-tagged and mutant bestrophin-1 (Best-1-ΔPxxP). The precipitation of β4-subunits using antibodies against c-Myc resulted in precipitates which were analyzed for the presence of bestrophin-1 (Best-1-ΔPxxP; 64 kDa) which was found in the precipitates (Fig. 5A). However, Best-1-ΔPxxP showed much weaker co-precipitation with β4-subunits. In the next set of experiments the effects of the mutant bestrophin-1 on L-type channels currents was investigated (Fig. 5B–F). Cells which express $Ca_V1.3$, β4-subunit and Best-1-ΔPxxP showed weak L-type channel currents with a significant lower current density (4.2 ± 0.6 $pApF^{-1}$, $n = 6$, $p = 0.047$; Fig. 5F). All properties of L-type channel currents with mutant bestrophin-1 were indistinguishable from those with wild-type bestrophin-1 ($n = 6$; voltage of half-maximal activation: $p = 0.32$; activation time constant at +20 mV: $p = 0.89$; Table 1). Analysis of the subcellular localization of all three proteins using confocal microscopy showed less presence of Best-1-ΔPxxP in the membrane as it was also indicated by a lower cytosol to membrane ratio of 2.4 compared to 4.8 of the wild-type (Fig. 5G 5H). Using pixel analysis of the fluorescence signals of Best-1-ΔPxxP and β4-subunits resulted in a Pearson's correlation coefficient 31.4% which indicate less co-localization of Best-1-ΔPxxP with Ca^{2+} channel proteins compared to wild-type bestrophin-1.

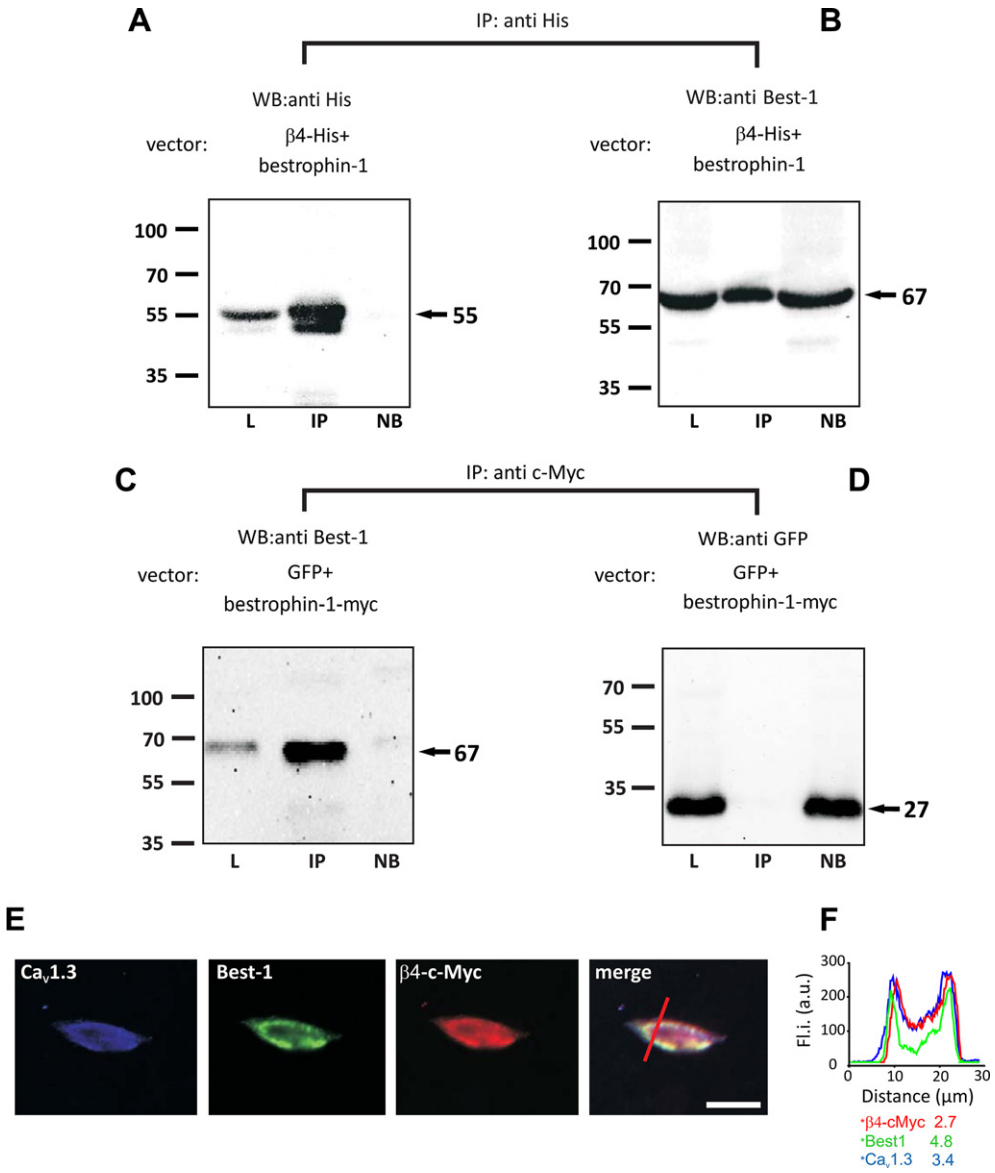

Fig. 2. Protein–protein interaction of β4-subunit and bestrophin-1. 2A: Anti-His staining of a Western-blot of precipitates obtained using cobalt-beads to precipitate His-tagged β4-subunits. Lysates are from HEK cells transduced with bestrophin-1 and His-tagged β4-subunits. Note: upper band is the specific β4-subunit staining. 2B: Bestrophin-1 staining of a Western-blot of the precipitates shown in 2A. Identification of bestrophin-1 in indicates co-precipitation of β4-subunit (55 kDa) and bestrophin-1 (67 kDa). 2C: Control of precipitation: bestrophin-1 stained Western-blot of precipitates obtained using antibodies against c-Myc; HEK transduction with GFP and bestrophin-1-c-Myc-tagged. 2D: Western-blot of the same precipitates stained against GFP (27 kDa) indicates no unspecific co-precipitation. 2E: Confocal pictures of CHO cells expressing bestrophin-1, β4-subunit, α2δ-subunit and $Ca_V1.3$ after patch-clamp analysis. 2F: Fluorescence profiles scanned along the red line in the merged picture, colors correspond with colors in confocal pictures; numbers give the ratio between cytosolic and membrane staining. Fl.i. a.u. = Fluorescence intensity, arbitrary units. Scale bar represents 10 μm (L = lysate; NB = nonbound fraction precipitation; IP = immunoprecipitation). (For the interpretation of the reference to color in this figure legend the reader is referred to the web version of this article.)

4. Discussion

This is the first study examining the effects of full length bestrophin-1 on the predominant L-type channel in RPE cells: human $Ca_V1.3$ channels and β4-subunits. We found that bestrophin-1 and $Ca_V1.3$ subunits co-localize in the cell membrane of the RPE, that bestrophin-1 binds to β4-subunits via a proline-rich motif/SH3 interaction, and that this binding accelerates time-dependent activation and decreases the activity of L-type channel currents. These effects could explain the changes in the light-peak amplitude of several mouse models. Moreover, they increase our understanding of the mechanism underlying altered function of the RPE caused by mutations in the bestrophin-1 gene.

The L-type channels in RPE cells are composed of $Ca_V1.3$ and by one of the β1,2,4-subunits (Rosenthal et al., 2006; Wimmers et al., 2008). Since β4-subunit deficient mice show decreased light-peaks (Marmorstein et al., 2006), we concentrated on the analysis of $Ca_V1.3$ subunits co-expressed with β4-subunits. Currents arising from the expression of $Ca_V1.3$, β4-subunits and α2δ subunits show a voltage-dependent activation shifted towards more negative voltages. Basically, these effects are in accordance with other publications examining the function of β-subunits in Ca^{2+} channels (Hanlon and Wallace, 2002; Kobayashi et al., 2007; Rousset et al., 2005). They are known to enhance the channel activity and modulate voltage-dependence, as well as kinetic behavior, of the Ca_V-subunit. The effects of β4-subunits on human $Ca_V1.3$ subunits have not been investigated to date, and reveal a new feature of this interaction. The shift in voltage-dependence to more negative membrane potentials is of functional relevance for L-type channels in RPE cells. L-type channels are high-voltage activated (HVA)

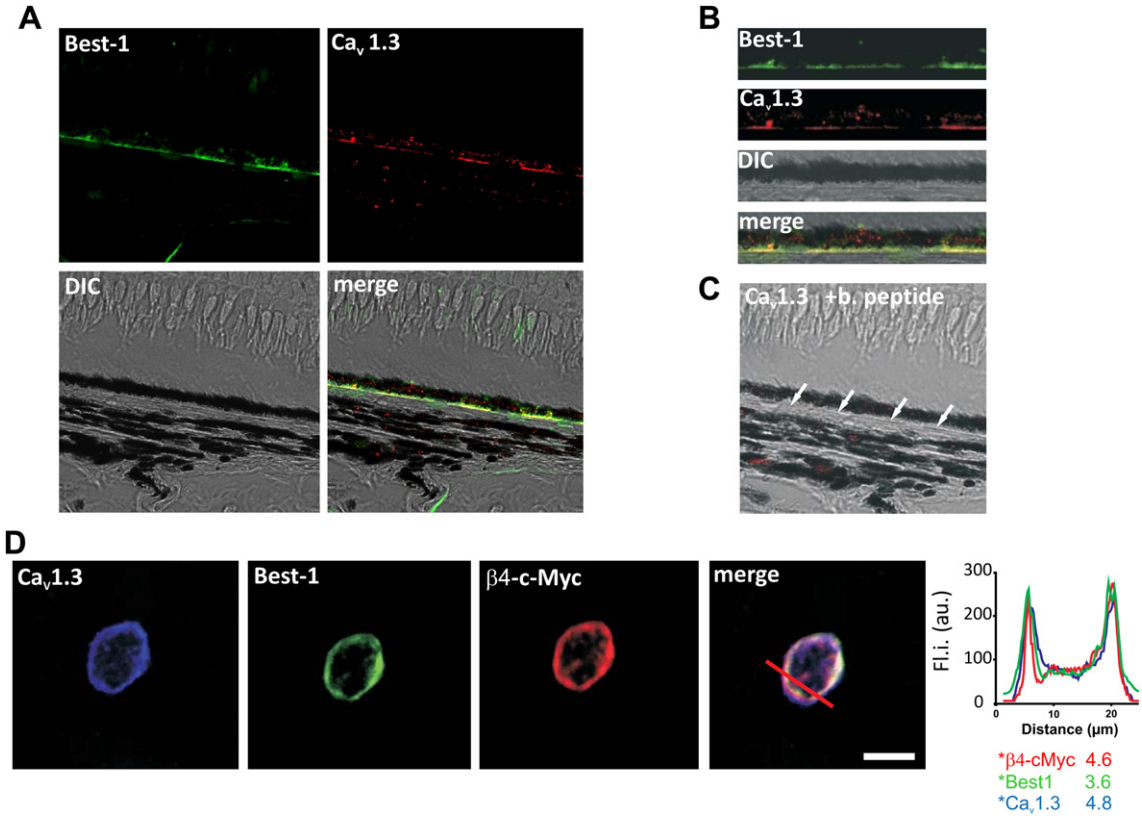

Fig. 3. Co-localization of Ca^{2+} channel subunits and bestrophin-1 in the RPE. 3A Cryosections of the porcine retina: Upper left panel: Immunostaining with antibodies against bestrophin-1. Upper right panel: Immunostaining with antibodies against $Ca_V1.3$. Lower left panel: light micrograph. Lower right panel: Overlay picture. (DIC = differential interference contrast). 3B: The RPE at higher magnification: basolateral localization of bestrophin-1 and $Ca_V1.3$ subunits. 3C: Negative control staining: $Ca_V1.3$ subunit antibody was pre-incubated with blocking peptide. 3D: Confocal pictures of ARPE-19 cells expressing bestrophin-1, β4-subunit, α2δ-subunit and $Ca_V1.3$ after patch-clamp analysis. Right panel, the fluorescence profiles are given for each protein measured along the red line in the merged picture, colors correspond with colors in confocal pictures; numbers give the ratio between cytosolic and membrane staining. Fl.i. a.u. = Fluorescence intensity, arbitrary units. Scale bar represents 10 μm.

channels, which usually activate at rather positive voltages. Thus a shift in the voltage-dependence towards more negative values, i.e. closer to the resting potential of RPE cells, is essential for the functional impact of L-type channels on RPE cells (Wimmers et al., 2007). Indeed analysis of the voltage-dependence of L-type channels in RPE cells revealed rather negative voltage-dependent activation (Rosenthal et al., 2006).

Recent publications reporting L-type channel modulation by bestrophin-1 reported changes in the current density, time-dependent activation or voltage-dependent activation (Burgess et al., 2008; Rosenthal et al., 2006; Yu et al., 2008). Thus, for the analysis of L-type channel properties, we concentrated on these parameters. When $Ca_V1.3$ was co-expressed with β3-subunits and bestrophin-1 no changes in the electrophysiological properties of the channel were observed. However, in contrast, when β4-subunits were co-expressed with bestrophin-1, the time-dependent activation of the L-type channel currents was accelerated at voltages between 0 and 20 mV. Additionally, the current density was reduced, which indicates a reduction of L-type channel activity. The reduction in the current density is in accordance to a study which used rat $Ca_V1.3$ subunits together with β1-subunits (Yu et al., 2008). Thus, the modulation of L-type Ca^{2+} channel activity depends on the β-subunit, with which bestrophin-1 interacts. This conclusion could help to understand the discrepancies between the two previous studies examining the effect of bestrophin-1 on L-type Ca^{2+} channel activity, as they used different β-subunits. When using β1-subunits, the main effects of bestrophin-1 were inhibition of the L-type channel currents (Yu et al., 2008). However, when co-expressed with β2-subunits the bestrophin-1 effect on $Ca_V1.2$ channel currents was an acceleration of the time-dependent activation (Burgess et al., 2008).

In order to find the molecular basis for Ca^{2+} channel modulation by bestrophin-1, immunoprecipitation experiments were performed. In contrast to earlier studies (Yu et al., 2008), we used the full length bestrophin-1. Both β4- and β3-subunits could be co-precipitated with bestrophin-1. Thus bestrophin-1 is able to physically bind to these β-subunits. This was confirmed by subcellular localization analysis using confocal microscopy. Cultured RPE cells showed the presence of $Ca_V1.3$, β4-subunit and bestrophin-1 in the cell membrane. Furthermore, in fresh sections of the porcine retina $Ca_V1.3$ subunits and bestrophin-1 co-localize in the basolateral membrane of the RPE. In our hands, the available antibodies against β4-subunits did not result in reliable staining of sections of the retina for immuno histochemistry. Thus, in heterologeous expression, and in native tissue, bestrophin-1 and L-type channels form interacting complexes. The identification of $Ca_V1.3$ as protein of the basolateral membrane is in accordance with experiments examining the influence of L-type channels on the light-peak amplitude. In these experiments, systemic application of the L-type channel blocker nimodipine resulted in a decreased light-peak amplitude (Rosenthal et al., 2006). This can only be explained by the presence of L-type channels in the RPE basolateral membrane because nimodipine only reaches the retina via the blood stream. Unaltered amplitudes of the a- and b-wave indicated that nimodipine did not pass the blood/retina barrier (Rosenthal et al., 2006).

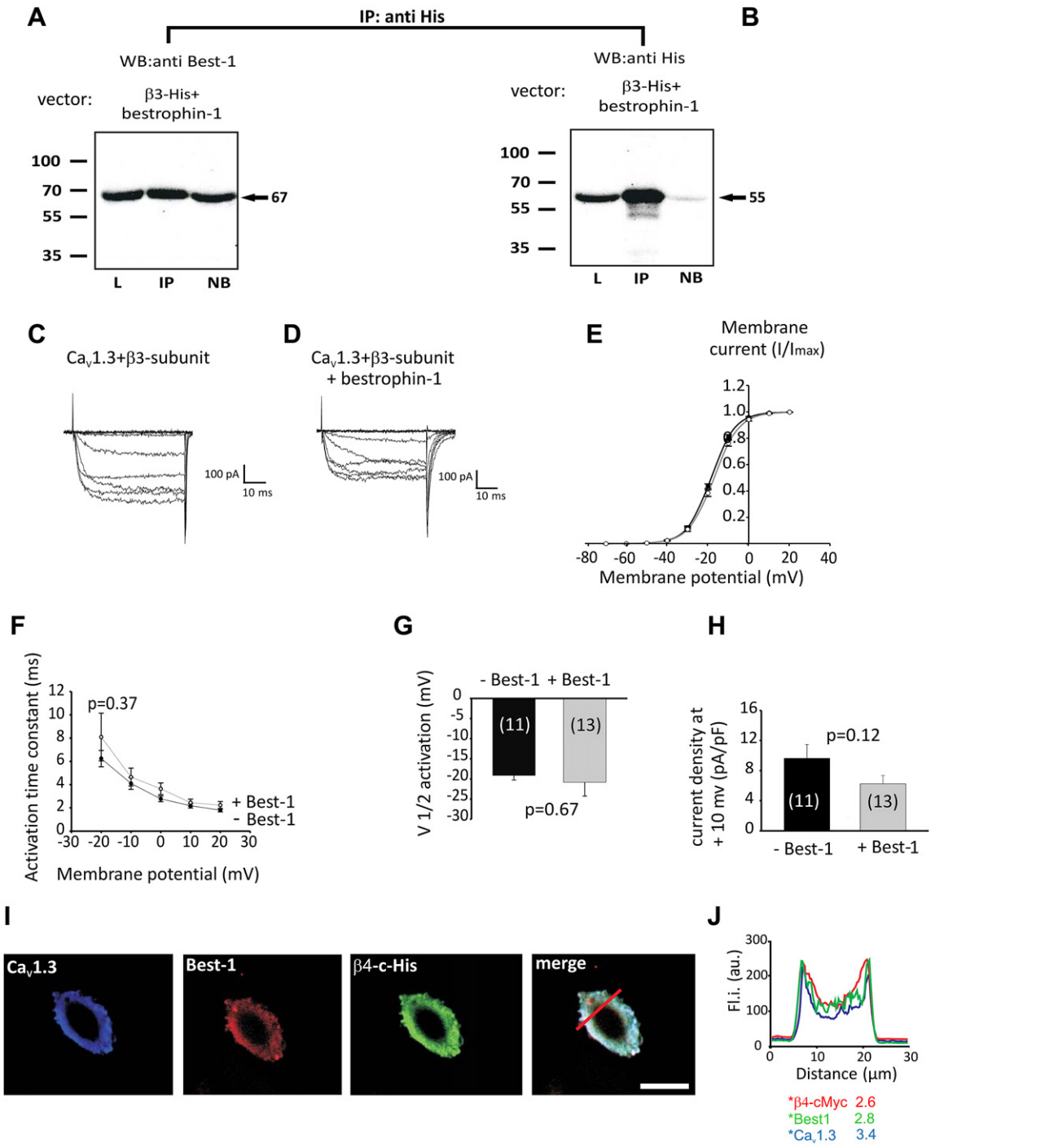

Fig. 4. Interaction of β3-subunits and bestrophin-1. 4A: Anti-bestrophin-1 (67 kDa) staining of a Western-blot of precipitates obtained using cobalt-beads to precipitate His-tagged β3-subunits (55 kDa). Lysates are from HEK cells which have been transduced with bestrophin-1 and His-tagged β3-subunits. 4B: Anti-His staining of a Western-blot of the same precipitates in 4A 4C: Ba^{2+} currents in CHO cells through $Ca_V1.3$ subunits (microinjection: $Ca_V1.3$ subunit, β3-subunit, α2δ-subunit); cells were electrically stimulated by the same stimulation as in 1A. 4D: Ba^{2+} currents in CHO cells through $Ca_V1.3$ subunits with bestrophin-1 (microinjection: $Ca_V1.3$ subunit, β3-subunit, α2δ-subunit, bestrophin-1); cells were stimulated by the stimulation as in 1A. 4E: Analysis of voltage-dependent activation: steady-state current amplitudes in the absence or presence of bestrophin-1 were plotted against the membrane potentials; curves were fitted using the Boltzmann equation. 4F: Analysis of time-dependent activation: time-dependent activation was measured by single exponential fit of the current activation with or without bestrophin-1. 4G: Comparison of voltage-dependent activation between the presence and the absence of bestrophin-1: voltage of half-maximal activation obtained from Boltzmann fits 4H: Comparison of current densities of the maximal current amplitude in the presence or in the absence of bestrophin-1. 4I: Confocal pictures of a CHO cell expressing bestrophin-1, β3-subunit, α2δ-subunit and $Ca_V1.3$ after patch-clamp analysis. In the right panel: Fluorescence profiles scanned along the red line in the merged picture, colors correspond with colors in confocal pictures; numbers give the ratio between cytosolic and membrane staining. Fl.i. a.u. = Fluorescence intensity, arbitrary units. Scale bar represents 10 μm (numbers in columns depict number of experiments; L = lysate; NB = nonbound fraction of precipitation; IP = immunoprecipitation).

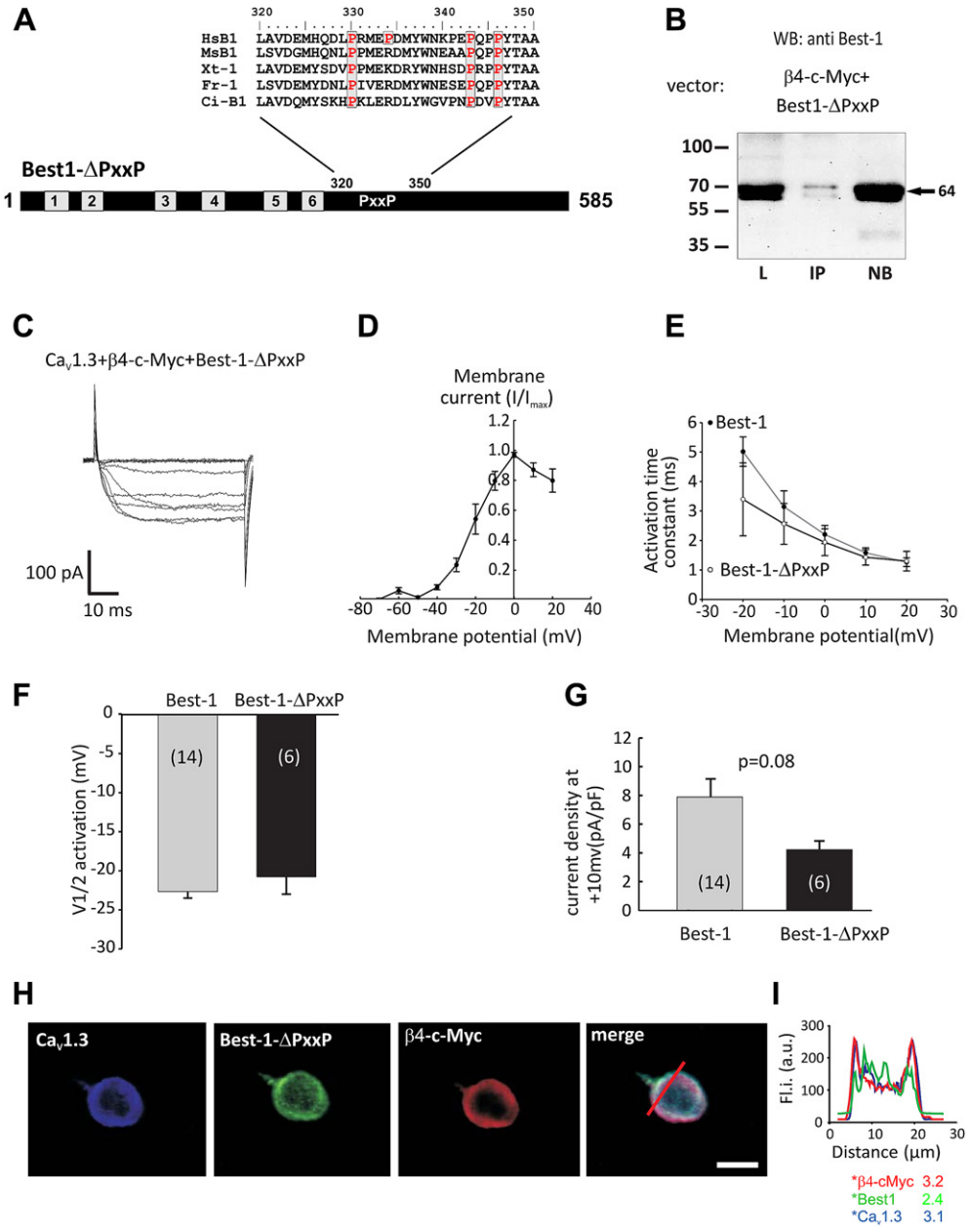

Fig. 5. β4-subunit interaction with bestrophin-1 lacking PxxP motifs (Best-1-ΔPxxP) at the amino acid positions 330 and 346. 5A: Schematic depiction of the Best-1-ΔPxxP construct used in this study and alignment of amino acid sequences of the conserved PxxP motif of the bestrophin-1 from different species. Boxes represent putative transmembrane domains (TMD). In the Best-1-ΔPxxP 30 amino acids (aa 320–350) containing conserved proline-rich motives were removed by site-directed mutagenesis. The following species abbreviations were used: Hs, Homo sapiens, Ms, Mus musculus, Xt, Xenopus tropicalis, Fr, Fugu rubripes, and Ci, Ciona intestinalis. 5B: Anti-bestrophin-1 staining of a western-blot of precipitates obtained using antibodies against c-Myc to precipitate c-Myc-tagged β4-subunits (55 kDa). Lysates are from HEK cells which have been transduced with Best-1-ΔPxxP and c-Myc-tagged β4-subunits. Note: upper band is mutant bestrophin-1 (64 kDa). 5C: Ba^{2+} currents in CHO cell through $Ca_V1.3$ subunits with Best-1-ΔPxxP (microinjection: $Ca_V1.3$ subunit, β4-subunit, α2δ-subunit, Best-1-ΔPxxP); cells were stimulated by the stimulation as in 1A. 5D: Analysis of voltage-dependent activation: steady-state current amplitudes were plotted against the membrane potentials; curves were fitted using the Boltzmann equation, comparison of currents in the presence of wild-type bestrophin-1 and Best-1-ΔPxxP. 5E: Analysis of time-dependent activation: time-dependent activation was measured by single exponential fit of the current activation; comparison of wild-type bestrophin-1 and Best-1-ΔPxxP. 5F: Comparison of voltage-dependent activation with wild-type bestrophin-1 and with Best-1-ΔPxxP: voltage of half-maximal activation obtained from Boltzmann fits. 5G: Comparison of current densities of the maximal current amplitude with wild-type bestrophin-1 or Best-1-ΔPxxP. 5H: Confocal pictures of CHO cells expressing Best-1-ΔPxxP, β4-subunit, α2δ-subunit and $Ca_V1.3$ after patch-clamp analysis. 5I: Fluorescence profiles scanned along the red line in the merged picture, colors correspond with colors in confocal pictures; numbers give the ratio between cytosolic and membrane staining. Fl.i. a.u. = Fluorescence intensity, arbitrary units. Scale bar represents 10 μm (numbers in the columns depict the number of experiments; L = lysate; NB = nonbound fraction of precipitation; IP = immunoprecipitation).

Using truncated forms of bestrophin-1, a cluster of proline-rich motifs on the C-terminus was detected which enable the modulation of L-type channel currents and binding of bestrophin-1 to β1-subunits (Yu et al., 2008). Since all Ca^{2+} channel β-subunits contain SH3-domains, the binding occurs via a proline-rich motif/SH3-domain interaction (Striessnig, 1999). In the present study we used a different approach:site-directed mutagenesis. With this technique, we removed a cluster of proline-rich motifs between amino acid position 330 and 346 on the C-terminus of bestrophin-1. This mutant showed reduced co-immuno precipitation with β4-subunit and less co-localization in the confocal analysis; indicating weaker binding affinity between the two proteins. This

resulted in a strongly reduced Ca^{2+} channel activity; although all L-type properties were indistinguishable from those with wild-type bestrophin-1. These results demonstrate a novel mechanism by which bestrophin-1 influences β-subunit function. β-subunits are not only responsible to modify electrophysiological properties of the pore-forming $Ca_V1.3$ subunit, they also are required to guide the Ca_V-subunits to the cell membrane (Hanlon and Wallace, 2002; Kobayashi et al., 2007; Rousset et al., 2005). The mutant bestrophin-1, with a lower affinity for β-subunits, alters the chaperone function of the β-subunits. If the disturbed interaction between bestrophin-1 and β-subunits can have such a severe effect on the activity of Ca^{2+} channels in the RPE, then it would be interesting to determine whether other disease-leading mutations would influence the chaperone function of β-subunits, too. Thus, we conclude that a reduced binding of mutant bestrophin-1, which lacks the proline-rich motifs in its C-terminus, reduces the trafficking of bestrophin-1 into the cell membrane and to a reduction of Ca^{2+}-channel activity.

The effect of the β4-subunit on Ca^{2+} channel activity possibly explains observations made in DC-electroretinography analysis of the light-peak amplitude in the mouse. Since $Ca_V1.3$ knock-out mice showed a decreased light-peak, the generation of this signal is dependent on these ion channels (Wu et al., 2007). The β4-subunit enhances the activity of L-type channels by acceleration of the activation time. In accordance with this, the β4-subunit deficient mouse showed decreased amplitudes of the light-peak (Marmorstein et al., 2006). On the other hand, mice lacking bestrophin-1 showed increased light-peak amplitudes at lower light-intensities (Marmorstein et al., 2006). This can be explained by the consequence of the bestrophin-1/β4-subunit interaction, which results in a reduced activity of the L-type channels. Such an inhibitory effect of bestrophin-1 is absent in bestrophin-1 knock-out mice, and therefore, would lead to larger light-peaks. An analysis of the DC-electroretinogram light-peak in W93C-bestrophin-1 knock-in mice was published recently (Zhang et al., 2010). Mice carrying this bestrophin-1 mutation also showed decreased light-peak amplitude, which was due to decreased intracellular Ca^{2+}-signals. Thus it is likely that this mutation reduced the ability of bestrophin-1 to stimulate L-type channels. We have previously shown that the W93C-bestrophin-1 mutation reduced the time-dependent activation of L-type channels in RPE-J cell line (Rosenthal et al., 2006).

In summary, we have demonstrated that full length bestrophin-1 binds to, and modulates, the Ca^{2+} channel proteins that are expressed in the RPE: $Ca_V1.3$ and β4-subunits. These channels are known to have a large influence on the light-peak amplitude of the EOG. These findings add further support to the hypothesis that bestrophin-1-induced L-type channel modulation in the RPE is of critical importance for RPE function. The interaction of bestropin-1 with β-subunits modifies two functions of β-subunits: the electrophysiological properties of L-type channels and maintenance of Ca^{2+} channel activity. A reduction of L-type channel activity in RPE cells would influence essential functions such as regulation of secretion or phagocytosis. Thus the consequences of interaction between mutant forms of bestrophin-1 and $Ca_V1.3$ channels reported in the present study, help us to understand the clinical picture of Best's disease: a decrease in the light-peak and retinal degeneration due to altered RPE function.

Acknowledgements

The authors greatly acknowledge the technical support of Elfriede Eckert, Andrea Danullis and Stefanie Schlichting. We gratefully thank Prof. Dr. Joerg Striessnig, Institute of Molecular Pharmacolgy, Innsbruck, for providing the expression vectors for Ca^{2+} channels, Prof. Karl Kunzelmann (Regensburg) for providing the bestrophin-1 antibodies. The authors want to thank to Dr. Miriam Breunig, Pharmazeutische Technologie, Regensburg for providing access to confocal microscope. We would like to especially thank Dr. David Slattery for helping us to improve the English language. The work was supported by Deutsche Forschungsgemeinschaft DFG grants STR480/9-1 and STR480/9-2, FOR1075, Gertrud-Kusen Stiftung.

References

Abramoff, M.D., Magelhaes, P.J., Ram, S.J., 2004. Image processing with image. J. Biophotonucs. Int. 11, 36–43.
Best, F., 1905. Über eine hereditäre Maculaaffection: Beiträge zur Vererbungslehre. Z. Augenheilkunde 13, 199–212.
Boon, C.J., Klevering, B.J., Leroy, B.P., Hoyng, C.B., Keunen, J.E., den Hollander, A.I., 2009. The spectrum of ocular phenotypes caused by mutations in the BEST1 gene. Prog. Retin. Eye Res. 28, 187–205.
Burgess, R., Millar, I.D., Leroy, B.P., Urquhart, J.E., Fearon, I.M., De Baere, E., Brown, P.D., Robson, A.G., Wright, G.A., Kestelyn, P., Holder, G.E., Webster, A.R., Manson, F.D., Black, G.C., 2008. Biallelic mutation of BEST1 causes a distinct retinopathy in humans. Am. J. Hum. Genet. 82, 19–31.
Hanlon, M.R., Wallace, B.A., 2002. Structure and function of voltage-dependent ion channel regulatory beta subunits. Biochemistry 41, 2886–2894.
Hartzell, H.C., Qu, Z., Yu, K., Xiao, Q., Chien, L.T., 2008. Molecular physiology of bestrophins: multifunctional membrane proteins linked to best disease and other retinopathies. Physiol. Rev. 88, 639–672.
Karl, M.O., Kroeger, W., Wimmers, S., Milenkovic, V.M., Valtink, M., Engelmann, K., Strauss, O., 2008. Endogenous Gas6 and Ca2+ -channel activation modulate phagocytosis by retinal pigment epithelium. Cell Signal. 20, 1159–1168.
Kobayashi, T., Yamada, Y., Fukao, M., Tsutsuura, M., Tohse, N., 2007. Regulation of Cav1.2 current: interaction with intracellular molecules. J. Pharmacol. Sci. 103, 347–353.
Marmorstein, L.Y., Wu, J., McLaughlin, P., Yocom, J., Karl, M.O., Neussert, R., Wimmers, S., Stanton, J.B., Gregg, R.G., Strauss, O., Peachey, N.S., Marmorstein, A.D., 2006. The light peak of the electroretinogram is dependent on voltage-gated calcium channels and antagonized by bestrophin (best-1). J. Gen. Physiol. 127, 577–589.
Marquardt, A., Stohr, H., Passmore, L.A., Kramer, F., RiveraA.Weber, B.H., 1998. Mutations in a novel gene, VMD2, encoding a protein of unknown properties cause juvenile-onset vitelliform macular dystrophy (Best's disease). Hum. Mol. Genet. 7, 1517–1525.
Petrukhin, K., Koisti, M.J., Bakall, B., Li, W., Xie, G., Marknell, T., Sandgren, O., Forsman, K., Holmgren, G., Andreasson, S., Vujic, M., Bergen, A.A., McGarty-Dugan, V., Figueroa, D., Austin, C.P., Metzker, M.L., Caskey, C.T., Wadelius, C., 1998. Identification of the gene responsible for Best macular dystrophy. Nat. Genet. 19, 241–247.
Rosenthal, R., Bakall, B., Kinnick, T., Peachey, N., Wimmers, S., Wadelius, C., Marmorstein, A., Strauss, O., 2006. Expression of bestrophin-1, the product of the VMD2 gene, modulates voltage-dependent Ca2+ channels in retinal pigment epithelial cells. Faseb J. 20, 178–180.
Rosenthal, R., Heimann, H., Agostini, H., Martin, G., Hansen, L.L., Strauss, O., 2007. Ca2+ channels in retinal pigment epithelial cells regulate vascular endothelial growth factor secretion rates in health and disease. Mol. Vis. 13, 443–456.
Rousset, M., Cens, T., Charnet, P., 2005. Alone at last! New functions for Ca2+ channel beta subunits? Sci. STKE 2005, pe11.
Strauss, O., 2005. The retinal pigment epithelium in visual function. Physiol. Rev. 85, 845–881.
Striessnig, J., 1999. Pharmacology, structure and function of cardiac L-type Ca(2+) channels. Cell. Physiol. Biochem. 9, 242–269.
Wimmers, S., Coeppicus, L., Rosenthal, R., Strauss, O., 2008. Expression profile of voltage-dependent Ca2+ channel subunits in the human retinal pigment epithelium. Graefes Arch. Clin. Exp. Ophthalmol. 246, 685–692.
Wimmers, S., Karl, M.O., Strauss, O., 2007. Ion channels in the RPE. Prog. Retin. Eye Res. 26, 263–301.
Wu, J., Marmorstein, A.D., Striessnig, J., Peachey, N.S., 2007. Voltage-dependent calcium channel CaV1.3 subunits regulate the light peak of the electroretinogram. J. Neurophysiol. 97, 3731–3735.
Yu, K., Xiao, Q., Cui, G., LeeA.Hartzell, H.C., 2008. The best disease-linked Cl- channel hBest1 regulates Ca V 1 (L-type) Ca2+ channels via src-homology-binding domains. J. Neurosci. 28, 5660–5670.
Zhang, Y., Stanton, J.B., Wu, J., Yu, K., Hartzell, H.C., Peachey, N.S., Marmorstein, L.Y., Marmorstein, A.D., 2010. Suppression of Ca2+ signaling in a mouse model of Best disease. Hum. Mol. Genet. 19, 1108–1118.

Untersuchung molekularer Grundlagen der Bestrophin-1/Ca^{2+}-Kanal-Interaktion

Zusammenfassung der zur Promotion vorgelegten Publikation:
Reichhart et al. 2010, Exp. Eye Res. 91: 630-39

Einleitung:

Die Best'sche vitelliforme Makuladystrophie (Morbus Best) ist eine hereditäre Form der Retinadegeneration (Best, F.; 1905), die mit der Akkumulation von Lipofuszin im Bereich des zentralen Anteils des retinalen Pigmentepithels assoziiert ist, welche sich in der Fundoskopie als die typische eidotterähnliche Läsion auf der Makula erkennen lässt. Als Leitsymptom und entscheidendes Kriterium für die Diagnose des Morbus Best gilt die Reduktion des Lichtanstieges im Elektro-Okulogramm der Patienten, einem Signal, dass durch die Aktivierung von Cl^- Kanälen im retinalen Pigmentepithel entsteht .Bestrophin-1, Genprodukt des krankheits- verursachenden Gens BEST1 (Marquardt et al., 1998; Petrukhin et al., 1998) ist im retinalen Pigmentepithel exprimiert (Marmorstein et al, 2000 und 2009). Somit lässt sich zusammengefasst der Morbus Best als eine Erkrankung des retinalen Pigmentepithels definieren. Das retinale Pigmentepithel spielt eine unter anderem eine wichtige Rolle bei der Lichtabsorption, dem Sehzyklus, der Phagozytose von Photorezeptoraußensegmenten, der Sekretion von Wachstumsfaktoren, sowie dem epithelialen Transport zwischen Retina und Choroidea und ist daher für die Aufrechterhaltung der Sehfunktion essentiell (Strauss, 2005). Das heißt, eine Fehlfunktion des retinalen Pigmentepithels durch BEST1 Mutationen kann als Ursache für die Photorezeptordegeneration und die Erblindung der Patienten

angesehen werden. Bestrophin-1 kann sowohl als Calcium-abhängiger Chloridkanal als auch als Regulator spannungsabhängiger L-Typ-Kanäle im retinalen Pigmentepithel fungieren (Hartzell et al., 2008). Mäuse mit einem genetischen Defekt, der zur Defizienz der Ca^{2+}-Kanal- β4-Untereinheiten führt (Wu et al., 2007) oder spannungsabhängigen L-Typ-Kanal (Ca_v1.3Untereinheit) defiziente Mäuse (Marmorstein et al., 2006), zeigen eine Verminderung des Lichtanstiegs im DC-ERG. Daher besteht die Hypothese, dass Bestrophin-1 abhängige Regulation der L-Typ-Kanalaktivität für die Änderungen im Lichtanstieg verantwortlich ist.

So wurde im Rahmen meiner Dissertation die regulatorische Funktion von Bestrophin-1 auf die Poren-formende Ca_V1.3-Untereinheit und zusätzlich auf die β4-Untereinheit spannungsabhängiger Ca^{2+}-Kanäle analysiert.

Material und Methoden

Material

Folgende Plasmide wurden verwendet:

1. Bestrophin-1, BEST-1 [Homo sapiens; NM_004183], hBest-pcDNA3.1
2. CACNB4, Calciumkanal, spannungsabhängig, L-Typ, β4-Untereinheit [Rattus norvegicus; Gene ID 58942] β4-pCDNA3
3. CACNB3, Calciumkanal, spannungsabhängig, L-Typ, β3-Untereinheit[Rattus norvegicus; Gene ID 25297], β3-pCMV
4. CACNA1D, Calciumkanal, spannungsabhängig, L-Typ, α1D subunit Ca_V1.3 (Homo sapiens: NM_000720.2)
5. α2δpcDNA3 (Gene ID 776)

6. eGFP pcDNA3 reporter plasmid was used as transduction control.

Zunächst wurden die β3- und die β4-Untereinheit in einen pCDNA3.1(+) Vektor mit C-myc oder 6xHis kloniert, um die Detektion der β-Untereinheiten mittels Antikörper zu vereinfachen. Hierfür wurden mittels PCR die Restriktionsenzymschnittstellen von KpnI und AgeI (New England Biolabs) an des Beginn bzw das Ende der Sequenz hinzugefügt.

Folgende Primer kamen zur Verwendung:

für β3: 5´-ACGGGTACCATGTATGACGACTCCTAC

5´-CGTACCGGTGTAGCTGTCCTTAGGCCA

und für β4: 5`- ACGGGTACCACCATGTCGTCCTCCTACGCC

5`-CGTACCGGTAAGCCTATGTCGGGAGTC

Die PCR-Produkte anschließend verdaut und in den mit denselben Restriktionsenzymen vorbereiteten Vektor ligiert.

Die Deletion des Prolin-reichen Aminosäure-Clusters im Bereich des C-Terminus vom humanen Bestrophin-1 erfolgte mittels Site-Directed Mutagenesis:

5´-ACGGGTACCCCACCATGACCATCACTTACACA;

5´-CGTACCGGTGGAATGTGCTTCATCCCT;

5´-AGGAATTTGCAGGTGTCCCTGGAATTCTCA;

5´-GTGCATCTCATCCACAGCCAAGAATTCTGA

Die beiden daraus resultierenden PCR-Produkte wurden mit den Restriktionsenzymen KpnI/EcoRI bzw. EcoRI/AgeI verdaut und in einen mit KpnI/AgeI geschnittenen pCDNA3.1(+) Vektor ligiert. Anschließende Sequenzierung ergab eine vollständige Deletion des Prolin-reichen Clusters zwischen den Aminosäuren 320-350.

Heterologe Expression

Basis sämtlicher Experimente war die heterologe Expression der Calciumkanaluntereinheiten sowie Bestrophin-1 in etablierten Zellkultursystemen. CHO (chinese hamster ovaries)-Zellen(ATCC, cat# CCL-61) wurden in in Ham's F-12 Medium (Invitrogen) kultiviert, HEK(human embryonic kidney)-293 Zellen (ATCC, cat# CRL-1573)in Dulbecco's modifiziertem Eagle's Medium(D-MEM), welches L-Glutamin, 4500 mg/l Glucose und110 mg/l Natrium- Pyruvat enthält, und ARPE(arising retinal pigment epithelia)- 19- Zellen (ATCC, cat# CRL-2302) in DMEM/Ham's F-12 medium (1:1 Verhältnis). Dieses wurde zusätzlich mit Insulin/Transferrin, nicht-essenziellen Aminosäuren und
15 mM HEPES (Invitrogen) versetzt. Zu allen Medien wurde noch 10% (v/v) fetales Kälberserum (Invitrogen), und 1% (v/v) Penicillin/Streptomycin (Invitrogen) hinzugefügt. Die Zellen wurden bei 37 ° C, bei relativer Luftfeuchte von 95% und 5% CO_2 Gehalt kultiviert.

Zur heterologen Expression wurden die subkonfluenten HEK-293-Zellen (ca. 70-80% konfluent) für Western Blot mit Satisfection Transduction Reagent (Stratagene) entsprechend dem Standardprotokoll des Herstellers transfiziert. Für die Immunhistochemie und die Patch Clamp Experimente wurden ARPE-19 respektive CHO-Zellen auf Glasscoverslips ausplattiert und durch Mikroinjektion mit dem Micromanipulator Inject-Man NI2 (Eppendorf) und dem Injektor FemtoJet (Eppendorf) transduziert, um die Expression von mehreren Plasmide gleichzeitig zu gewährleisten. Hierzu wurde jedes Plasmid in einer Konzentration von 50 ng/µl verwendet. Anschließend wurden die Zellen für 24-48h bei 30°C, relativer Luftfeuchte

von 95% und 5% CO_2 Gehalt inkubiert, um eine optimale Expression der α1D-Untereinheit zu erreichen.

Immunopräzipitation

Zur Untersuchung der physikalischen Interaktion zwischen Bestrophin-1 und den β-Untereinheiten kam Immunopräzipitation mit jeweils 50 μl HisPur Cobalt Resin (Pierce) zur Immunopräzipitation von Proteinen mit 6xHis-Tag oder Protein G-Agarose-beads (Roche) und relevantem Primärantikörper und anschließend Western Blot zur Verwendung. Hierfür wurden subkonfluente HEK-Zellen zunächst mit β-Untereinheit oder GFP als Kontrolle und WT Bestrophin-1 bzw. der Deletionsmutante transfiziert und nach 36h mit einem Puffer, bestehend aus folgenden Komponenten, lysiert:
150 mM TrisHCl, pH 7.5, 150 mM NaCl, 1% Nonidet-P40, 0.5% Natriumdeoxycholat. Als Proteaseinhibitor diente Roche Complete Mini. Die Protein G beads wurden zunächst mit 5-10μl des primären Antikörpers (mouse anti-c-Myc (9E10)(Developmental Studies Hybridoma Bank) für die Immunopräzipitation vorinkubiert. Nach Inkubation der Zelllysate mit den Cobalt-beads respektive den mit Antikörper versetzten Protein G-beads über Nacht bei 4°C wurden die Proben dreimal unter Verwendung eines Puffers mit folgender Zusammensetzung gewaschen: 50 mM Tris-HCl, pH 7.5, 150 mM NaCl, 1% Nonidet-P40, 0.5% Natrium-Deoxycholat, sowie zusätzlich 10 mM Imidazol bei Verwendung der His Pur Cobalt Resin.

Sämtliche Zentrifugationsschritte erfolgten bei 1200xg bei 4°C. Anschließend wurden die Proben mit 4xSDS Ladepuffer sowie 150mM Imidazol für die IP mit den Cobalt

beads bzw. mit 0.5µl β-Mercaptoethanol für die Proben mit den ProteinG-beads versetzt und bei 90°C für 3min erhitzt, um eine Dissoziation der mit Antikörper beladenen Proteinkomplexe von den beads zu erwirken.Nach Durchführung einer SDS-Page mit einem 10% SDS-Gel, das mit den Lysaten (L), den Immunopräzipitations-Proben (IP) und den nicht gebundenen Fraktionen (NB) beladen wurde, wurden die Proteine auf eine PVDF Filter Membran (GE Healthcare) geblottet und mit PBS-Tween, versetzt mit 5% Magermilchpulver für 30 min inkubiert. Nach Inkubation mit dem entsprechenden primären Antikörper (mouse monoklonal anti-human bestrophin-1, ab2182, (Abcam plc), anti-bestrophin-1 Antikörper (von Prof. Dr. Karl Kunzelmann zur Verfügung gestellt), rabbit anti-Ca_VBeta3 (Alomone Labs), goat anti Ca_V1.3 (Santa Cruz), mouse anti-c-Myc (9E10)(Developmental Studies Hybridoma Bank), rabbit anti-6His, ab9108, (Abcam plc), mouse monoclonal anti-GFP (Roche) über Nacht und einstündiger Inkubation mit HRP(horse radish peroxidase)-konjugierten goat anti-rabbit oder goat anti-mouse Antikörper(New England Biolabs) wurden die Proteine mittels eines ECL-Kits (Pierce) gemäß Anleitung visualisiert und mittels eines Imagingsystems (ChemiImager, Biozym) digitalisiert.

Immunohistochemie

Die Analyse der Lokalisation von Bestrophin-1 und den β-Untereinheiten erfolgte mittels konfokaler Mikroskopie nach immunhistochemischer Färbung. Hierfür wurden die mittels Mikroinjektion vorbereiteten Zellen nach 36h Inkubation zunächst mit 4% (w/v) Paraformaldehyd für 10min bei Raumtemperatur fixiert. Nach drei Waschschritten mit 1xPBS wurden die Zellen für 30 min mit einer „Blocking Solution“ permeabilisiert, die sich aus folgenden Komponenten zusammensetzte: 10% (v/v) Ziegenserum, 0.5% (v/v) Triton X-100 in 1x PBS.

Anschließend wurden die fixierten Zellen über Nacht bei 4°C mit dem Primärantikörper inkubiert. Hierzu wurden folgende Antikörper verwendet:

- mouse monoclonal anti-bestrophin antibody, ab2182, (Abcam plc),
- goat polyclonal anti $Ca_v1.3$, sc-16251 (Santa Cruz),
- rabbit polyclonal anti-cmyc,ab32072 (Abcam plc) ,
- rabbit polyclonal anti-Caβ3 antibody, ACC-008 (AlomoneLabs)

jeweils in einer Verdünnung von 1:500 in 2% Ziegenserum mit 0.1% Triton X-100 in 1xPBS. Nach drei weiteren Waschschritten mit 1xPBS und etwa einstündiger Inkubation mit dem spezifischen fluoreszeierenden sekundären Antikörpern Alexa Fluor 488, Alexa Fluor 546, and Alexa Fluor 633 (Invitrogen) sowie Hoechst 33342 (Invitrogen) zum Staining des Nucleus. Die konfokalen Bilder wurden quantitativ ausgewertet mithilfe der ImageJ Software (Abramoff et al., 2004). Pearson's Korrelationskoeffizient(PCC) wurde zur Analyse der Kolokalisation verwendet.

Patch-Clamp Untersuchungen der $Ca_V1.3$ Kanalaktivität

Die $Ca_V1.3$-Aktivität wurde mit Hilfe der Patch-Clamp Methode nach vorhergehender Mikroinjektion, untersucht. Hierfür bestand die Extrazellulärlösung aus folgenden Komponenten (in mM): Cholinchlorid 150, $BaCl_2$ 10, $MgCl_2$ 1, HEPES 10; der pH wurde mit CsOH auf 7.4 eingestellt. Somit ergab sich eine Osmolarität von 333mOsm. Direkt vor dem Gebrauch wurde die Extrazellulärlösung noch mit 0.1% Glucose versetzt.

Die verwendete Pipettenlösung enthielt (in mM): CsCl 135, MgCl2 1, CsEGTA 10; der pH wurde mit CsOH auf 7.4 eingestellt. Die Osmolarität betrug 283mOsm.

Für die Patch Clamp Experimente wurde ein computergesteuerter EPC-10 Verstärker in Verbindung mit TIDA, einer Software zur Analyse der erhobenen Daten verwendet. Die mittlere Membranleitfähigkeit betrug 22.04 ±1.3 pF.

Der Zugangswiderstand wurde auf Werte unter 10MΩ kompensiert. Für die Analyse der spannungsabhängigen Aktivierung wurden die Ströme gegen die Membranpotentiale der elektrischen Stimulation geplottet. Plots von jeder Einzelzelle wurden mittels der Boltzmann Gleichung gefittet.
Die Statistische Auswertung erfolgte mittels univariater Varianzanalyse (ANOVA). Alle Daten wurden als Mittelwert ± Standard Error of the mean (SEM) angegeben, wobei * für statistische Signifikanz mit $p < 0.05$ steht.

Ergebnisse:

Präzipitation von β4-Untereinheiten führte zu Co-Immunopräzipitation mit Bestrophin-1. Als Negativkontrolle führte die Präzipitation von Bestrophin-1 in Zellen, die nur mit Bestrophin-1 und GFP in Abwesenheit der β-Untereinheit transfiziert wurden zu keiner Co-Immunopräzipitation. Die darauf folgende Analyse der subzellulären Lokalisation zeigte Kolokalisation von Bestrophin-1, $Ca_V1.3$ und in der Zellmembran. Die Bestimmung Pearson's Correlation Coefficient zwischen Bestrophin-1 und β4-Untereinheit ergab 85%.

$Ca_V1.3$ Ströme in Abwesenheit von Bestrophin-1 zeigten für L-Typ-Kanäle typische Potentialabhängigkeit, Kinetik und Stromdichte (Koschak et al 2001). Bei $Ca_V1.3$/β-4 L-Typ Kanälen zeigte sich In der Gegenwart von Bestrophin-1eine beschleunigte zeit-abhängige Aktivierung und eine verminderte Stromdichte verglichen mit Strömen, die in Abwesenheit von Bestrophin-1 gemessen wurden. Die spannungsabhängige Aktivierung blieb unverändert. In Anwesenheit der β3-

Untereinheit, welche nicht im RPE exprimiert ist, modulierte Bestrophin-1 die $Ca_V1.3$-Aktivität nicht.

Die Deletion eines hochkonservierten Clusters Prolin-reicher Motive im Bereich des C-Terminus(Aminosäure 320-350) von Bestrophin-1 reduzierte die Co-Immunopräzipitationseffizienz mit der β4-Untereinheit und verringerte die $Ca_V1.3$-Aktivität deutlich. Zellen die $Ca_V1.3$-Untereinheit und Bestrophin-1, welchem die Prolin-reichen Motive fehlen, koexprimieren, zeigten einen gestörten und somit weniger effizienten zielgerichteten zytosolischen Transport von Bestrophin-1 in die Zellmembran, was sich in einem deutlich verminderten Pearson's Correlation Coefficient von 31% zwischen der Bestrophin-1-Mutante und β4-Untereinheit widerspiegelte.

Diskussion:

Zusammenfassend lässt sich aus den Ergebnissen folgern, dass Bestrophin-1 auf Basis einer molekular definierten Interaktion als Ca^{2+}-Kanal-Interaktionspartner betrachtet werden kann. In dieser Interaktion wirkt es auf die Funktion der β-Untereinheiten, welche im Wesentlichen in der Modulation der Porenaktivität und der Regulation der Oberflächenexpression des Calciumkanalkomplexes besteht. Das von uns analysierte Prolin-reiche Cluster beeinflusst im Wesentlichen die Funktion der Regulation der $Ca_V1.3$-Oberflächenexpression. Wie bereits bekannt ist, haben $Ca_V1.3$-Kanäle einen Einfluss auf die Amplitude des Lichtanstiegs im EOG und sind essentiell für die homöostatischen Funktionen des RPE (Strauss, O.; 2005). Die hier

untersuchte Bestrophinmutante zeigt, dass wild-typisches Bestrophin-1 die Verfügbarkeit dieser Kanäle in der Zellmembran reguliert. Die Ergebnisse meiner Studie zeigen, dass die Regulation der $Ca_V1.3$-Kanäle im RPE ein wesentliches Element der Regulation der RPE Zellfunktion sein kann, das durch krankheitsbedingte Mutationen gestört werden kann. Somit stellen diese Daten einen neuen Schritt dahingehend dar, die Verringerung des Lichtanstiegs bei Patienten mit Morbus Best und die Alteration des RPE, die letztendlich zur retinalen Degeneration führen, zu erklären.

Referenzen:

Abramoff, M.D., Magelhaes, P.J., Ram, S.J., 2004. Image processing with image. J. Biophotonics. Int. 11, 36-43.

Best, F.; 1905. Über eine hereditäre Maculaaffection: Beiträge zur Vererbungslehre. Z. Augenheilkunde 13, 199-212

Hartzell, H. C., Qu, Z., Yu, K., Xiao, Q.Chien, L. T.; 2008. Molecular physiology of bestrophins: multifunctional membrane proteins linked to best disease and other retinopathies. Physiol. Rev. 88, 639-72

Koschak A, Reimer D, Huber I, Grabner M, Glossmann H, et al. 2001. Alpha 1D ($Ca_v1.3$) subunits can form l-type Ca^{2+} channels activating at negative voltages. J Biol Chem 276: 22100–22106.

Marmorstein A.D., Marmorstein, L.Y., Rayborn M., Wang X., Hollyfield J.G., Petrukhin K., Bestrophin, the product of the Best vitelliform macular dystrophy gene (*VMD2*), localizes to the basolateral plasma membrane of the retinal pigment epithelium. 2000, Proc Natl Acad Sci USA 97:12758-63.

Marmorstein, L. Y., Wu, J., McLaughlin, P., Yocom, J., Karl, M. O., Neussert, R., Wimmers, S., Stanton, J. B., Gregg, R. G., Strauss, O., Peachey, N. S., Marmorstein, A. D.; 2006. The light peak of the electroretinogram is dependent on voltage-gated calcium channels and antagonized by bestrophin (best-1). J. Gen. Physiol. 127, 577-89.

Marmorstein AD, Cross HE, Peachey NS. Functional roles of bestrophins in ocular epithelia. 2009 Prog Retin Eye Res.28:206-26.

Strauss, O.; 2005. The retinal pigment epithelium in visual function. Physiol. Rev. 85, 845-81.

Wu, J., Marmorstein, A. D., Striessnig, J.Peachey, N. S.; 2007. Voltage-dependent calcium channel $Ca_V1.3$ subunits regulate the light peak of the electroretinogram. J. Neurophysiol. 97, 3731-5.

Curriculum vitae

Name:	Nadine Reichhart
Geburtsdatum:	16.11.1985
Geburtsort:	München, Deutschland
Wohnort:	Kirchheim bei Tittmoning, Deutschland
Staatsbürgerschaft:	deutsch
Familienstand:	ledig

Schulen:

1992-1996	Grundschule in Tittmoning
1996-2005:	Rottmayr-Gymnasium in Laufen
09/2005	Abitur am Rottmayr-Gymnasium in Laufen (1,0)

Universitäre Laufbahn:

2005-2011	Studium der Humanmedizin an der Universität Regensburg
09/2007	1.Abschnitt der ärztlichen Prüfung
11/2011	2.Abschnitt der ärztlichen Prüfung (Gesamtnote:1,66)
19.02.2012	Approbation als Ärztin

Praktisches Jahr:

30.08.2010-19.12.2010 1.Tertial: Pathologie, Universitätsklinikum Regensburg
20.12.2010-10.04.2011 2.Tertial: Innere Medizin, GZO Wetzikon, Schweiz
11.04.2011-31.07.2011 3.Tertial: Chirugie, Caritas Krankenhaus St.Josef, Regensburg

Wissenschaftlicher Werdegang:

ab Mai 2008 Beginn der med. Promotion mit dem Thema: „Untersuchung molekularer Grundlagen der Bestrophin-1-/Ca^{2+}-Kanal-Interaktion“ (Experimentelle Ophthalmologie der Universitätsklinik Regensburg, Prof.Dr.O.Strauß)

04/2009-12/2011 SHK am Institut für experimentelle Ophthalmologie

02/2012-02/2013: wissenschaftliche Mitarbeiterin am Institut für experimentelle Ophthalmologie der Universitätsklinik Regensburg

Kongressteilnahme:

2009: Pro Retina Potsdam (Abstract: Interaction between Bestrophin-1 and β-subunits of Voltage dependent calcium channels)

2011: DPG Regensburg (Abstract: Effect of bestrophin-1 on L-type Ca2+ channel activity depends on interaction of proline-rich sites of bestrophin-1 with the Ca2+ channel β -subunit

Veröffentlichungen:

Reichhart N, Milenkovic VM, Halsband CA, Cordeiro S, Strauss O (2010). Effect of bestrophin-1 on L-type Ca2+ channel activity depends on the Ca2+ channel beta-subunit. Exp Eye Res. 91(5):630-9

Milenkovic VM, Krejcova S, Reichhart N, Wagner A, Strauss O (2011)Interaction of bestrophin-1 and Ca2+ channel β -subunits: identification of new binding domains on the bestrophin-1 C-terminus. PLoS One 29;6(4):e19364.

Danksagung

An dieser Stelle möchte ich mich bei allen danken, die mich bei meiner Promotion unterstützt haben, insbesondere:

Herrn Prof. Dr.rer.nat Olaf Strauß für die Möglichkeit in seiner Arbeitsgruppe eine Promotionsarbeit anfertigen zu dürfen, für die zahlreichen Diskussionen und die berufliche Förderung

Herrn Dr.rer.nat.Vladimir Milenkovic für die praktische Betreuung und Begleitung meiner Arbeit

Frau Andrea Dannullis, Frau Elfriede Eckert und Frau Renate Föckler für ihre unermüdliche Unterstützung und die Einführung in den Laboralltag

allen weiteren Mitglieder der Arbeitsgruppe, die ich während meiner Promotion kennengelernt habe, und jetzt nicht namentlich erwähne.

es war eine wunderbare Zeit, die ich auf keinen Fall missen möchte,

nicht zuletzt meinen Großeltern und Freunden, die mich in Zeiten der Frustration über die Tücken einer wissenschaftlichen Dissertation emotional stabilisiert haben und die ich vermutlich furchtbar genervt habe.